

Deflection Light Behaviors by AdS Black Holes

A. Belhaj*, H. Belmahi †, M. Benali ‡§

Département de Physique, Équipe des Sciences de la matière et du rayonnement, ESMaR

Faculté des Sciences, Université Mohammed V de Rabat

Rabat, Morocco

December 14, 2021

Abstract

We investigate the behavior of the deflection of light rays by charged and rotating AdS black holes using the Gauss-Bonnet formalism. Taking weak field approximations and certain appropriate limits associated with AdS geometries, we compute and analyze such an optical quantity by varying the involved moduli space parameters. First, we study the charge and the AdS radius effects on the deflection angle of RN-AdS black holes. For small values of the impact parameter b , we find that the charge effect is relevant. Precisely, it decreases the deflection angle, while the AdS background one is not. For large values of b , however, these optical behaviors have been inverted and the deflection angle becomes an increasing function of the charge. In this way, the cosmological constant effect is remarked to be relevant showing linear variations of the deflection angle. Varying the charge, we find a critical impact parameter value b_c where the charge effect is inverted. For rotating solutions, we show that the spinning parameter still decreases the deflection angle without any changing behavior observed in the charge effect. Evincing of the cosmological constant, we recover known results corresponding to charged and rotating ordinary black hole solutions. Examining the plasma effect, we reveal that the deflection angle keeps the same behavior being a decreasing function in terms of the frequency ratio.

Keywords: AdS black holes, Deflection angle analysis, Gauss-Bonnet theorem, Plasma medium.

*a-belhaj@um5r.ac.ma

†hajar_belmahi@um5.ac.ma

‡mohamed_benali4@um5.ac.ma

§Authors in alphabetical order.

Contents

1	Introduction	3
2	Deflection angle of light rays from Gauss-Bonnet formalism	4
3	Deflection angle behaviors by Reissner–Nordström AdS black holes	5
4	Deflection angle of Kerr-Newman AdS black holes	9
5	Plasma medium and deflection angle of light rays	12
6	Conclusions	15

1 Introduction

The investigation of black hole physics has received a relevant interest in connections with various gravity models in different dimensions [1–3]. The associated studies have been encouraged and supported by recent astrophysical observations [4–6]. Besides gravitational wave detections, this involves the imaging of a supermassive black hole candidate in the center of galaxy M87 provided by the Event Horizon Telescope (EHT) collaborations [7]. Concretely, black hole physical aspects have been considered as a rich subject being approached using various methods and roads based either on analytical or numerical computations. In particular, thermodynamic properties of AdS black holes have been extensively investigated by interpreting the cosmological constant as a pressure [8–10]. In this way, many transitions have been dealt with providing promising results [11, 12]. A special emphasis has been put on the Hawking-Page transition of a large class of AdS black holes in arbitrary dimensions in the presence of nontrivial backgrounds including dark energy and D-brane objects embedded in higher dimensional supergravity models [13–15]. This gives results corresponding to the second order phase transition between large black holes (LBH) and small black holes (SBH). A close examination shows that such a transition, based on the Gibbs free energy computations, has provided certain universalities in AdS black hole physics [16]. Moreover, optical behaviors of black holes have been also studied giving arise to interesting findings associated with shadow and deflection angle variations. In particular, it has been revealed that non-rotating black holes exhibit perfect circular geometries. The size of such shapes depends on black hole parameters including the mass, the charge and the stringy brane number [17–21]. These circular geometries have been distorted by implementing the rotating parameter generating non-trivial configurations called D-shapes, being controlled by astronomical observables describing the size and the shape geometric deformations [22]. Among others, Kerr solutions with certain approximations could bring results matching with EHT collaborations [23]. In paralleled studies, the deflection angle of light rays has been also investigated. This optical quantity could unveil certain data which may impose particle physics constraints associated with black hole detections. In particular, many works on such optical aspects have been conducted [24–28]. An inspection shows that this optical quantity has been approached using different methods. Precisely, Gibbons and Werner have proposed a direct method to compute the deflection angle using the Gauss-Bonnet theorem. This method, which will be used in the present paper, is based on backgrounds relying on a space metric [29, 30]. It is worth noting, in passing, that other methods have been exploited including the one based on the elliptic integral formalism combined with equations of motion [31]. Concretely, it has been explored a link between the deflection angle and the thermodynamic behaviors of AdS black holes [32]. Approaching the deflection angle of black holes could bring new insights in the associated black hole physics.

The aim of this paper is to contribute to these activities by investigating the deflection angle variations of certain charged and rotating AdS black holes. This could support the recent findings which combine the thermodynamic and the deflection angle behaviors [32].

Using the Gauss-Bonnet formalism, we compute and numerically analyze the deflection angle of AdS black hole solutions in terms of the involved physical parameters including the refractive index. Analyzing the behavior of RN-AdS deflection angle, we show that for small values of the impact parameter b , the charge effect is relevant. Concretely, it decreases the deflection angle while the cosmological constant one is not. For large values of b , however, these aspects have been inverted. In this way, the cosmological constant effect becomes relevant showing linear variations of the light deflection angle. Moreover, the charge increases the deflection angle. For non-rotating solutions, we observe a specific point where the deflection angle behavior gets changed around a critical value of the impact parameter denoted by b_c . Moving to the rotating case, we find that the rotating parameter decreases the deflection angle without any critical inverted point. In the absence of the cosmological constant, we recover known results corresponding to charged and rotating ordinary black hole solutions. Inspecting the plasma effect, we find that the deflection angle keeps the same behavior described by a decreasing function in terms of the frequency ratio.

This work is structured as follows. In section 2, we give a concise review on deflection angle computations using the Gauss-Bonnet formalism. In section 3, we investigate the deflection angle behaviors of charged AdS black holes. Section 4 concerns the study of charged and rotating AdS black holes. In section 4, we extend such results by considering the plasma medium effect. The last section is devoted to conclusions and open questions.

2 Deflection angle of light rays from Gauss-Bonnet formalism

In this section, we present the formalism being needed to examine behaviors of the deflection angle of certain AdS black holes in four dimensions. A close inspection reveals that there are, a priori, many ways to evaluate such an optical quantity. One of them is based on the geodesic equations of motion controlling the dynamics of the studied black holes. This method, however, brings solutions in terms of complicated elliptic functions [25, 31]. The second method, which will be exploited here, relies on the Gauss-Bonnet theorem and optic metric computations [33]. Considering the observer and the source at finite distance in the equatorial plane, the deflection angle can be expressed as

$$\Theta = \Psi_R - \Psi_S + \phi_{SR}, \quad (2.1)$$

where Ψ_R and Ψ_S are angles between the light rays and the radial direction at the observer and the source position, respectively. ϕ_{SR} is the longitude separation angle [33]. The computation of the deflection angle can be elaborated by exploiting the Gauss-Bonnet theorem [29]. Indeed, the associated relation is given by

$$\iint_{\Sigma} K dS + \sum_{\alpha=1}^n \int_{C_{\alpha}} k_g dl + \sum_{\alpha=1}^n \theta_{\alpha} = 2\pi, \quad (2.2)$$

where Σ is a two dimensional orientable real surface bounded by curves $C_\alpha (\alpha = 1, \dots, n)$. θ_α indicates the external angle at the α -vertex. K is the Gaussian curvature of the surface Σ and k_g represents the geodesic curvature of C_α . By considering the quadrilateral ${}_r^\infty \square_S^\infty$ formed of light curves from the source to the observer, it has been shown that Eq.(2.1) and Eq.(2.2) provide a reduced integral formula on the space geometry which reads

$$\Theta = - \iint_{{}_r^\infty \square_S^\infty} K dS + \int_S^R k_g dl. \quad (2.3)$$

It is noted that dS is the area element of the involved surface. The line element dl can be handled by considering axisymmetric black holes with the following metric form

$$ds^2 = -A(r, \theta)dt^2 + B(r, \theta)dr^2 + C(r, \theta)d\theta^2 + D(r, \theta)d\phi^2 - 2H(r, \theta)dtd\phi. \quad (2.4)$$

To defined the Riemannian manifold for which the light geodesics are interpreted as spatial curves, we should exploit the null geodesic condition $ds^2 = 0$ [33]. Indeed, this gives

$$dt = \pm \sqrt{\gamma_{ij} dx^i dx^j} + \eta_\phi d\phi, \quad (2.5)$$

where γ_{ij} is a spatial metric. In the equatorial plane ($\theta = \pi/2$) at constant t of the space-time metric, one has a 2-dimensional curved space which is represented by

$$dl^2 \equiv \gamma_{ij} dx^i dx^j. \quad (2.6)$$

In this way, the Gaussian curvature is expressed as follows

$$K = \frac{R_{r\phi r\phi}}{\gamma} = \frac{1}{\sqrt{\gamma}} \left(\frac{\partial}{\partial \phi} \left(\frac{\sqrt{\gamma}}{\gamma_{rr}} \Gamma_{rr}^{\phi} \right) - \frac{\partial}{\partial r} \left(\frac{\sqrt{\gamma}}{\gamma_{rr}} \Gamma_{r\phi}^{\phi} \right) \right), \quad (2.7)$$

where one has used $\gamma = \det(\gamma_{ij})$. The area element of the Eq.(2.2) takes the form

$$dS = \sqrt{\gamma} dr d\phi. \quad (2.8)$$

According to [33], the geodesic curvature in this Riemannian manifold is given by

$$k_g = - \frac{1}{\sqrt{\gamma \gamma^{\theta\theta}}} \eta_{\phi,r}. \quad (2.9)$$

Having presented the associated calculations, we move now to investigate certain optical aspects of AdS black holes by computing the corresponding deflection angle. Concretely, we approach such an optical quantity by varying the involved parameters in different backgrounds.

3 Deflection angle behaviors by Reissner–Nordström AdS black holes

In this section, we are interested in deflection angle behaviors of charged solutions called Reissner–Nordström AdS (RN-AdS) black holes in four dimensions. Indeed, the line element

of the corresponding space-time metric is written as

$$ds^2 = -f(r)dt^2 + \frac{dr^2}{f(r)} + r^2(d\theta^2 + \sin^2(\theta)d\phi^2), \quad (3.1)$$

where $f(r)$ indicates the metric function given by $f(r) = 1 - \frac{2M}{r} + \frac{r^2}{\ell^2} + \frac{Q^2}{r^2}$. M and Q represent the mass and the charge of AdS black holes, respectively. ℓ is the AdS radius linked to four dimensional cosmological constant via the following relation

$$\Lambda = -\frac{3}{\ell^2}. \quad (3.2)$$

Applying the null geodesic conditions in the equatorial plane, one gets the optical metric expression

$$dt^2 = \frac{1}{f(r)^2}dr^2 + \frac{r^2}{f(r)}d\phi^2. \quad (3.3)$$

Using Eq.(2.7) and Eq.(3.3), the Gaussian curvature takes the form

$$K \simeq \frac{1}{\ell^2} - \frac{6M}{\ell^2 r} + \frac{6Q^2}{\ell^2 r^2} - \frac{2M}{r^3} + \frac{3Q^2}{r^4} - \frac{6MQ^2}{r^5} + O(M^2, Q^3, 1/\ell^4). \quad (3.4)$$

In this case, the determinant of the optical metric can be expressed as follows

$$\gamma = r^2 \left(1 - \left(\frac{2M}{r} - \frac{r^2}{\ell^2} - \frac{Q^2}{r^2} \right) \right)^{-3} \quad (3.5)$$

which provides the following needed approximation

$$\sqrt{\gamma} \simeq r + O(M^1, Q^2, 1/\ell^2). \quad (3.6)$$

To keep the order $O(M^2, Q^3, 1/\ell^4)$ in deflection angle computations, we use the Eq.(3.6). Indeed, the computation gives

$$\begin{aligned} \int_{\phi_S}^{\phi_R} \int_{r_o}^{\infty} K \sqrt{\gamma} dr d\phi &\simeq \int_{\phi_S}^{\phi_R} \int_{r_o}^{\infty} dr d\phi \left(\frac{r}{\ell^2} + \frac{3Q^2}{r^3} + \frac{6Q^2}{\ell^2 r} - \frac{6M}{\ell^2} - \frac{2M}{r^2} - \frac{6MQ^2}{r^4} \right) \\ &+ O(M^2, Q^3, 1/\ell^4) \end{aligned} \quad (3.7)$$

where r_o is the distance of the closest approach corresponding to the solution of the orbit equation. To develop such computations, the impact parameter of motion is needed. It is given by

$$b = \frac{|L|}{E} = \frac{r^2}{f(r)} \frac{d\phi}{dt}, \quad (3.8)$$

where E and L are the two constants of motion. Putting $u = \frac{1}{r}$, the null geodesic condition gives

$$\left(\frac{du}{d\phi} \right)^2 = \frac{1}{b^2} - \frac{1}{\ell^2} - u^2 (-2Mu + Q^2 u^2 + 1). \quad (3.9)$$

To solve the second derivation of Eq.(3.9), we should use the perturbative method which provides that

$$u(\phi) = \frac{1}{b} \sin(\phi) + O(M). \quad (3.10)$$

In the weak field approximations and for small values of the AdS radius, the integral of Eq.(3.7) can be expanded as follows

$$\begin{aligned} - \int_{\phi_S}^{\phi_R} \int_{r_o}^{\infty} K \sqrt{\gamma} dr d\phi &\simeq \int_{\phi_S}^{\phi_R} \int_0^{u(\phi)=\frac{1}{b} \sin(\phi)} 2M - 3Q^2 u + 6MQ^2 u^2 - \frac{1}{\ell^2 u^3} + \frac{6M}{\ell^2 u^2} - \frac{6Q^2}{\ell^2 u} du d\phi \\ &\simeq \frac{2M}{b} \left[\sqrt{1 - (bu_S)^2} + \sqrt{1 - (bu_R)^2} \right] \\ &+ \left[\frac{6Q^2}{\ell^2} - \frac{3Q^2}{4b^2} \right] \left[\pi - \arcsin(bu_S) - \arcsin(bu_R) \right] \\ &- \frac{3Q^2}{4b^2} \left[bu_R \sqrt{1 - (bu_R)^2} + bu_S \sqrt{1 - (bu_S)^2} \right] \\ &- \frac{MQ^2}{3b^3} \left[(16 + (bu_R)^2) \sqrt{1 - (bu_R)^2} + (16 + (bu_S)^2) \sqrt{1 - (bu_S)^2} \right] \\ &+ \frac{b}{2\ell^2} \left[\frac{\sqrt{1 - (bu_R)^2}}{u_R} + \frac{\sqrt{1 - (bu_S)^2}}{u_S} \right] - \frac{Mb}{2\ell^2} \left[\frac{1}{\sqrt{1 - (bu_S)^2}} + \frac{1}{\sqrt{1 - (bu_R)^2}} \right] \\ &- \frac{6Q^2 b}{\ell^2} \left[u_S \arctan(u_S b) + u_R \arctan(u_R b) \right], \end{aligned} \quad (3.11)$$

where u_S and u_R are the inverse of the source and the observer distance. In this case, where the coefficient $H(r, \theta)$ of the coupling term $dt d\phi$ is missed, it has been observed that the second term of the deflection angle expression associated with k_g takes a vanishing value. The integral of Eq.(3.11) can apparently diverge in the limit $bu_S \rightarrow 0$ and $bu_R \rightarrow 0$. This divergence could be linked to the cosmological constant effect. Combining Eq.(3.11) and Eq.(2.3) and using the asymptotic case corresponding to $bu_S \ll 1$ and $bu_R \ll 1$, the deflection angle of the RN-AdS black hole is found to be

$$\Theta \simeq \frac{4M}{b} - \frac{3Q^2 \pi}{4b^2} - \frac{32MQ^2}{3b^3} + \frac{6Q^2 \pi}{\ell^2} - \frac{Mb}{\ell^2} + \frac{b}{2\ell^2} \left[\frac{1}{u_R} + \frac{1}{u_S} \right] + O(M^2, Q^3, 1/\ell^4). \quad (3.12)$$

An examination shows that one can make contact with known results. Putting $\ell \rightarrow \infty$, we recover, indeed, the expression of RN black holes [24, 34]. It has been observed that the expression of the deflection angle exhibits a divergent behavior associated with vanishing limits of u_S and u_R functions. Taking $Q = 0$, similar behaviors with the same terms of the AdS contributions have been found in [35] for $r_g = 2M$. Firstly, we examine the behavior of the deflection angle as a function of the impact parameter b in AdS backgrounds. Considering the expression of the deflection angle given by Eq.(3.12), the variation of such an optical quantity is illustrated in Fig.(1). Fixing the mass and the charge, we consider certain AdS radius values where their contributions will be relevant. It follows from this figure that the deflection angle decreases rapidly for small values of the impact parameter. Then, it increases by growing b . It is worth noting that similar behaviors have been obtained in [36]. Increasing

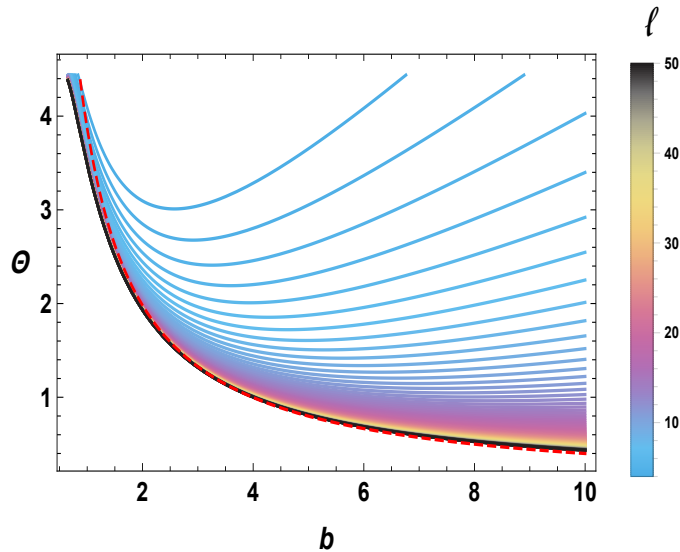


Figure 1: Variation of the deflection angle in terms of the impact parameter for different values of ℓ by taking $u_S = u_R = 0.1$, $M = 1$ and $Q = 0.2$. The dashed red curve represents the deflection angle of the Schwarzschild black hole.

the value of ℓ , the deflection angle decreases. It has been revealed that the presence of the AdS geometry could deviate the light rays. For small values of the impact parameter b , the deflection angle of the Schwarzschild black hole is a little large compared with the one corresponding to AdS contributions. Fixing $\ell = 50$ and taking large values of b , we remark the same behavior appearing in the deflection angle of the Schwarzschild black hole solution. For $\ell < 50$, the deflection angle in the presence of the cosmological constant becomes relevant. In the Fig(2), we inspect the charge effect on the deflection angle of RN AdS black holes. For small values of b , the deflection angle decreases by increasing the charge. This behavior has been inverted for large values of the impact parameter. However, the inverted behavior starts from a specific value of the impact parameter $b \simeq 8.716$ for $M = 1$ and $\ell = 20$. It follows from the figure that all Q curves meet at a critical point b_c . This means that this critical value should depend only on M and ℓ . A close examination shows that an explicit expression of b_c can be obtained by using the derivation of the deflection angle with respect to the charge. The computation gives

$$b_c = \frac{(\lambda\sqrt{6})^{2/3} + (6\pi)^{2/3}\ell^2}{12(\pi\lambda)^{1/3}} \quad (3.13)$$

where one has used $\lambda = (\sqrt{65536M^2\ell^4 - 6\pi^2\ell^6} + 256M\ell^2)$. It has been observed that this behavior changing of the deflection angle, in terms of the charge, appears in the case of the quintessential RN black hole [27]. However, this is removed in the case of RN ordinary black holes. These behaviors could be understood from the metric function $f(r)$ expression. For small values of b , the charge effect is notable while the cosmological constant one is not

relevant. In this case, we observe that the deflection angle involves a maximum. The letter is increasing by decreasing the charge Q . For large values of b , these properties have been inverted. Indeed, in this case, the cosmological constant effect becomes relevant showing linear variations of the deflection angle of light rays. We expect to obtain similar optical aspects for a large class of AdS black holes in four dimensions.

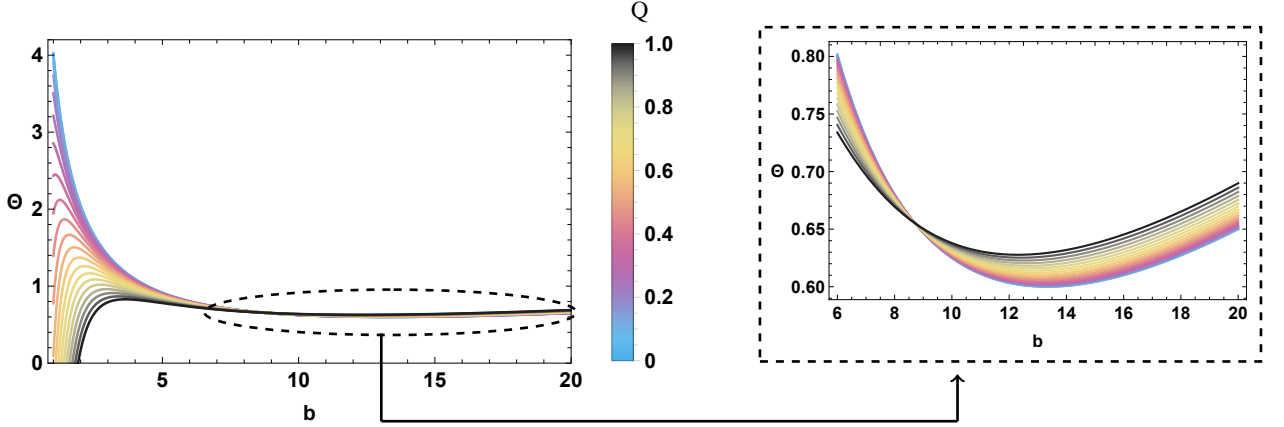


Figure 2: Variation of the deflection angle in terms of the impact parameter for different charge values by considering $u_S = u_R = 0.1$, $\ell = 20$ and $M = 1$.

4 Deflection angle of Kerr-Newman AdS black holes

Looking for the rotating parameter effect in the AdS geometry, we investigate the deflection angle of Kerr-Newman AdS black holes. According to [37], the line element of this class of black holes is given by

$$ds^2 = -\frac{\Delta_r}{\Sigma} \left[dt - \frac{a \sin^2 \theta}{\Xi} d\phi \right]^2 + \frac{\Sigma}{\Delta} dr^2 + \frac{\Sigma}{\Delta_\theta} d\theta^2 + \frac{\Delta_\theta \sin^2 \theta}{\Sigma} \left[a dt - \frac{r^2 + a^2}{\Xi} d\phi \right]^2, \quad (4.1)$$

where one has

$$\begin{aligned} \Sigma &= r^2 + a^2 \cos^2 \theta, \quad \Xi = 1 - \frac{a^2}{\ell^2}, \quad \Delta_\theta = 1 - \frac{a^2}{\ell^2} \cos^2 \theta \\ \Delta_r &= (r^2 + a^2) \left(1 + \frac{r^2}{\ell^2} \right) - 2Mr + Q^2. \end{aligned} \quad (4.2)$$

In the equatorial plane, the null geodesic condition yields to

$$\gamma_{rr} = \frac{r^4}{\left((a^2 + r^2) \left(\frac{r^2}{\ell^2} + 1 \right) - 2Mr + Q^2 \right) \left(r \left(\frac{r(a^2 + r^2)}{\ell^2} - 2M + r \right) + Q^2 \right)}, \quad (4.3)$$

$$\gamma_{\phi\phi} = \frac{l^6 r^4 (a^2 (\ell^2 + r^2) + \ell^2 (-2Mr + Q^2 + r^2) + r^4)}{(a^2 - \ell^2)^2 (r^2 (a^2 + r^2) + \ell^2 (r(r - 2M) + Q^2))^2}, \quad (4.4)$$

$$\eta_\phi = -\frac{a \ell^2 (r^2 (a^2 + r^2) + \ell^2 (Q^2 - 2Mr))}{(a^2 - \ell^2) (r^2 (a^2 + r^2) + \ell^2 (r(r - 2M) + Q^2))}. \quad (4.5)$$

In this model, the area element on the equatorial plane is found to be

$$dS \simeq r dr d\phi + O(M^1, Q^2, a^2, 1/\ell^2). \quad (4.6)$$

Considering the weak field and the slow rotation approximations with small values of the AdS radius, we can obtain the expression of the Gaussian curvature. Precisely, it is given by

$$\begin{aligned} K \simeq & \frac{1}{\ell^2} - \frac{6M}{\ell^2 r} + \frac{6Q^2}{\ell^2 r^2} - \frac{14a^2 M}{\ell^2 r^3} - \frac{2M}{r^3} + \frac{15a^2 Q^2}{\ell^2 r^4} + \frac{3Q^2}{r^4} - \frac{6MQ^2}{r^5} + \frac{24a^2 M}{\ell^2 r^5} - \frac{6a^2 M}{r^5} \\ & + \frac{8a^2 Q^2}{r^6} + \frac{12a^2 M Q^2}{r^7} + O\left(M^2, Q^3, a^2, \frac{1}{\ell^4}\right). \end{aligned} \quad (4.7)$$

Using Eq.(3.10), the integral calculation can be expanded as

$$\begin{aligned} - \int_{\phi_S}^{\phi_R} \int_{r_o}^{\infty} K \sqrt{\gamma} dr d\phi \simeq & \frac{2M}{b} \left[\sqrt{1 - (bu_S)^2} + \sqrt{1 - (bu_R)^2} \right] \\ & + \left[\frac{6Q^2}{\ell^2} - \frac{3Q^2}{4b^2} \right] \left[\pi - \arcsin(bu_S) - \arcsin(bu_R) \right] \\ & - \frac{3Q^2}{4b^2} \left[bu_R \sqrt{1 - (bu_R)^2} + bu_S \sqrt{1 - (bu_S)^2} \right] \\ & - \frac{MQ^2}{3b^3} \left[(16 + (bu_R)^2) \sqrt{1 - (bu_R)^2} + (16 + (bu_S)^2) \sqrt{1 - (bu_S)^2} \right] \\ & + \frac{b}{2\ell^2} \left[\frac{\sqrt{1 - (bu_R)^2}}{u_R} + \frac{\sqrt{1 - (bu_S)^2}}{u_S} \right] \\ & - \frac{Mb}{2\ell^2} \left[\frac{1}{\sqrt{1 - (bu_S)^2}} + \frac{1}{\sqrt{1 - (bu_R)^2}} \right] \\ & - \frac{6Q^2 b}{\ell^2} \left[u_S \arctan(u_S b) + u_R \arctan(u_R b) \right] + O\left(M^2, Q^3, a, \frac{1}{\ell^4}\right). \end{aligned} \quad (4.8)$$

To get the expression of k_g , one should exploit Eq(2.9). Indeed, the computations of the geodesic curvature give

$$k_g \simeq -\frac{2a}{\ell^2} - \frac{aM}{\ell^2 r} - \frac{2aM}{r^3} - \frac{3aMQ^2}{2\ell^2 r^3} + \frac{2aQ^2}{r^4} + \frac{3aMQ^2}{r^5} + O\left(M^2, Q^3, a, \frac{1}{\ell^4}\right). \quad (4.9)$$

For the prograde case where $dl > 0$, we consider $r = b/\cos\vartheta$ and $l = b\tan\vartheta$. This linear approximation of the photon is needed to get the integratio computations. In particular, we

obtain

$$\begin{aligned}
\int_S^R k_g dl &\simeq \int_S^R -\frac{2ab}{\ell^2 \cos^2 \vartheta} - \frac{aM}{\ell^2 \cos \vartheta} - \left[\frac{2aM}{b^2} + \frac{3aMQ^2}{2\ell^2 b^2} \right] \cos \vartheta + \frac{2aQ^2}{b^3} \cos^2 \vartheta + \frac{3aMQ^2}{b^4} \cos^3 \vartheta d\vartheta \\
&= -\frac{2a}{\ell^2} \left[\frac{\sqrt{1-(bu_R)^2}}{u_R} + \frac{\sqrt{1-(bu_S)^2}}{u_S} \right] + \frac{aQ^2}{b^3} [\pi - \arcsin(bu_S) - \arcsin(bu_R)] \\
&\quad - \frac{aM}{\ell^2} \left[\pi - \arctan(\sqrt{1-(u_S b)^2}) - \arctan(\sqrt{1-(u_R b)^2}) \right] \\
&\quad - \left[\frac{2aM}{b^2} + \frac{3aMQ^2}{2\ell^2 b^2} - \frac{2aMQ^2}{b^4} \right] \left[\sqrt{1-(bu_S)^2} + \sqrt{1-(bu_R)^2} \right] \\
&\quad + \frac{aQ^2}{b^2} \left[u_S \sqrt{1-(u_S b)^2} + u_R \sqrt{1-(u_R b)^2} \right] \\
&\quad + \frac{aMQ^2}{b^2} \left[u_S^2 \sqrt{1-(u_S b)^2} + u_R^2 \sqrt{1-(u_R b)^2} \right] + O\left(M^2, Q^3, a, \frac{1}{\ell^4}\right). \tag{4.10}
\end{aligned}$$

Combining Eqs.(4.9) and (4.10), the limits $bu_S \ll 1$ and $bu_R \ll 1$ provide

$$\begin{aligned}
\Theta_{KN_{AdS}} &\simeq \frac{4M}{b} - \frac{3Q^2\pi}{4b^2} - \frac{4aM}{b^2} - \frac{3aMQ^2}{\ell^2 b^2} - \frac{32MQ^2}{3b^3} + \frac{aQ^2\pi}{b^3} + \frac{4aMQ^2}{b^4} + \frac{6Q^2\pi}{\ell^2} - \frac{aM\pi}{2\ell^2} \\
&\quad - \frac{Mb}{\ell^2} + \left[\frac{b}{2\ell^2} - \frac{2a}{\ell^2} \right] \left[\frac{1}{u_R} + \frac{1}{u_S} \right] + O\left(M^2, Q^3, a, \frac{1}{\ell^4}\right). \tag{4.11}
\end{aligned}$$

From Eq.(4.11), we see that we can recover the rotating and the charge contribution terms obtained in the Kerr-Newman ordinary black holes [38]. Considering gravitational bending angle of lights for finite distances where the observer and the source location as $u_S = u_R = 0.1$, we illustrate the variation of the deflection angle Θ in terms of the impact parameter by varying the rotating parameter for fixed values of the mass, the charge and the AdS radius. These behaviors are plotted in Fig(3).

To explore the effect of the cosmological constant, we consider two specific AdS radius values. Indeed, we examine $\ell = \infty$ and $\ell = 20$ presented in left and right panels, respectively. In the absence of AdS backgrounds, the deflection angle decreases by increasing the rotating parameter a . It remains decreasing for generic values of b . The right panel of the figure shows that the deflection angle decreases rapidly for small values of b then it becomes an increasing function. Taking a generic value of ℓ , the deflection angle decreases with the rotation parameter. In the fixed charge solutions, however, the previous behavior changing point is not observed for the rotation parameter variation. It is worth noting that, in this case, the variation of the charge provides a critical point b_c^a where the charge effect is inverted. This critical point can be also obtained by using the deflection angle charge derivative. This value should depend on the three parameters ℓ , M and a . Indeed, the computation gives

$$b_c^a = b_c + a \left(\frac{\mu + \nu}{(6\pi)^{2/3} \lambda^{4/3} (3\pi^2 \ell^2 - 32768M^2)} \right) \tag{4.12}$$

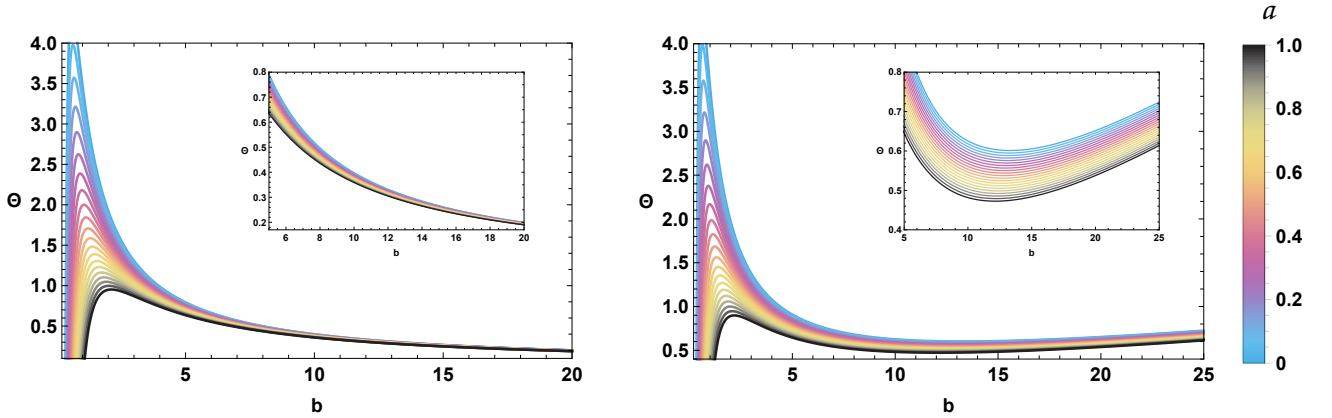


Figure 3: Variation of the deflection angle in terms of the impact parameter for different values of a by taking $u_S = u_R = 0.1$, $M=1$ and $Q = 0.2$. Left panel: behavior with $\ell = \infty$, right panel: behavior with $\ell = 20$.

where one has used

$$\begin{aligned}
 \mu &= -16777216\sqrt[3]{6}M^4\ell^2 - 65536\sqrt[3]{6}M^3(\lambda - 256M\ell^2) + 512M^2\left(256\pi^{4/3}\lambda^{2/3}\ell^2 - 253\sqrt[3]{6}\pi^2\ell^4\right) \\
 \nu &= \pi^{4/3}M(\lambda - 256M\ell^2)\left(515\lambda^{2/3} - 509\sqrt[3]{6}\pi^{2/3}\ell^2\right) + 12\sqrt[3]{6}\pi^4\ell^6 \\
 &\quad - 12\pi^{10/3}\lambda^{2/3}\ell^4(6\pi)^{2/3}\lambda^{4/3}(3\pi^2\ell^2 - 32768M^2).
 \end{aligned} \tag{4.13}$$

Sending a to zero, we recover the previous relation associated with non rotating solutions.

5 Plasma medium and deflection angle of light rays

In this section, we investigate the plasma effect on the weak deflection angle of four-dimensional AdS black holes. For simplicity reasons, we consider only the Kerr-Newman AdS solution by assuming that the calculations for other models can be done in a similar way. To do so, certain optical quantities are needed. According to [3], the refraction index in terms of the photon four-momentum and velocity u^B can be written as

$$n^2 = 1 + \frac{P_\alpha P^\alpha}{(P_B u^B)^2}. \tag{5.1}$$

For a non-magnetized cold plasma, Eq.(5.1) reduces to the following form

$$n^2 = 1 - \frac{\omega_p(r)^2}{\omega_0^2}, \tag{5.2}$$

where ω_0^2 represents the photon frequency and $\omega_p(p)$ is the electron plasma frequency. A priori, there are many models which have been dealt with. Here, however, we consider a

specific form studied in [39, 40]. Using a radial power law, the associated photon frequency can be written as follows

$$\omega_p^2(r) = \frac{k}{r^h}, \quad h > 0, \quad (5.3)$$

where k is an arbitrary constant being related to certain physical quantities. To inspect such an effect, we examine a concrete model relying on an inhomogeneous space-time. For the sake of simplicity, we take $h = 1$. In this way, the two dimensional optical geometry of the Kerr-Newman AdS black hole, in the presence of the plasma medium, is given by

$$dl = n^2 \gamma_{ij} dx^i dx^j, \quad (5.4)$$

being a generalized form of Eq.(2.6). This provides the following expression of the Gaussian optical curvature

$$\begin{aligned} K &= \frac{1}{\ell^2} + \left(-\frac{6M}{\ell^2} + \frac{3k}{2\omega_0^2 \ell^2} \right) \frac{1}{r} + \left(\frac{6Q^2}{\ell^2} + \frac{3k^2}{\omega_0^4 \ell^2} - \frac{15kM}{2\omega_0^2 \ell^2} \right) \frac{1}{r^2} \\ &+ \left(-2M + \frac{11k^3}{2\omega_0^6 \ell^2} - \frac{11k^2 M}{\omega_0^4 \ell^2} + \frac{7kQ^2}{\omega_0^2 \ell^2} + \frac{k}{2\omega_0^2} \right) \frac{1}{r^3} \\ &+ \left(3Q^2 + \frac{9k^4}{\omega_0^8 \ell^2} - \frac{33k^3 M}{2\omega_0^6 \ell^2} + \frac{9k^2 Q^2}{\omega_0^4 \ell^2} + \frac{3k^2}{2\omega_0^4} - \frac{9kM}{2\omega_0^2} \right) \frac{1}{r^4} \\ &+ \left(-6MQ^2 + \frac{27k^5}{2\omega_0^{10} \ell^2} - \frac{24k^4 M}{\omega_0^8 \ell^2} + \frac{12k^3 Q^2}{\omega_0^6 \ell^2} + \frac{3k^3}{\omega_0^6} - \frac{9k^2 M}{\omega_0^4} + \frac{9kQ^2}{2\omega_0^2} \right) \frac{1}{r^5} + O\left(M^2, Q^3, a, \frac{1}{\ell^2}\right). \end{aligned} \quad (5.5)$$

The first part of the deflection angle equation could be expanded as follows

$$\begin{aligned} - \int_{\phi_S}^{\phi_R} \int_{r_o}^{\infty} K \sqrt{\gamma} dr d\phi &= \left(2M - \frac{11k^3}{2\omega_0^6 \ell^2} + \frac{11k^2 M}{\omega_0^4 \ell^2} - \frac{7kQ^2}{\omega_0^2 \ell^2} - \frac{k}{2\omega_0^2} \right) \left(\frac{\sqrt{1 - (bu_S)^2} + \sqrt{1 - (bu_R)^2}}{b} \right) \\ &- \left(\frac{3Q^2}{4b^2} + \frac{9k^4}{\omega_0^8 \ell^2 4b^2} - \frac{33k^3 M}{8\omega_0^6 \ell^2 b^2} + \frac{9k^2 Q^2}{4\omega_0^4 \ell^2 b^2} + \frac{3k^2}{8\omega_0^4 b^2} - \frac{9kM}{8\omega_0^2 b^2} \right) \\ &\times \left([\pi - \arcsin(bu_S) - \arcsin(bu_R)] + \left[bu_R \sqrt{1 - (bu_R)^2} + bu_S \sqrt{1 - (bu_S)^2} \right] \right) \\ &+ \left(-6MQ^2 + \frac{27k^5}{2\omega_0^{10} \ell^2} - \frac{24k^4 M}{\omega_0^8 \ell^2} + \frac{12k^3 Q^2}{\omega_0^6 \ell^2} + \frac{3k^3}{\omega_0^6} - \frac{9k^2 M}{\omega_0^4} + \frac{9kQ^2}{2\omega_0^2} \right) \frac{1}{18b^3} \\ &\times \left[(16 + (bu_R)^2) \sqrt{1 - (bu_R)^2} + (16 + (bu_S)^2) \sqrt{1 - (bu_S)^2} \right] \\ &+ \frac{b}{2\ell^2} \left(\frac{\sqrt{1 - (bu_R)^2}}{u_R} + \frac{\sqrt{1 - (bu_S)^2}}{u_S} \right) + \left(-\frac{Mb}{2\ell^2} + \frac{kb}{8\omega_0^2 \ell^2} \right) \left(\frac{1}{\sqrt{1 - (bu_S)^2}} + \frac{1}{\sqrt{1 - (bu_R)^2}} \right) \\ &+ \left(\frac{6Q^2}{\ell^2} + \frac{3k^2}{\omega_0^4 \ell^2} - \frac{15kM}{2\omega_0^2 \ell^2} \right) ([\pi - \arcsin(bu_S) - \arcsin(bu_R)] - b [u_S \arctan(u_S b) + u_R \arctan(u_R b)]) \\ &+ O\left(M^2, Q^3, a, \frac{1}{\ell^2}\right). \end{aligned} \quad (5.6)$$

Moreover, the geodesic curvature is found to be

$$\begin{aligned}
k_g &= -\frac{2a}{\ell^2} + \left(-\frac{2ak}{\omega_0^2 \ell^2} - \frac{aM}{\ell^2}\right) \frac{1}{r} - \left(\frac{2ak^2}{\omega_0^4 \ell^2} + \frac{akM}{\omega_0^2 \ell^2}\right) \frac{1}{r^2} + \left(-2aM - \frac{2ak^3}{\omega_0^6 \ell^2} - \frac{ak^2 M}{\omega_0^4 \ell^2} - \frac{3aMQ^2}{2\ell^2}\right) \frac{1}{r^3} \\
&+ \left(2aQ^2 - \frac{2ak^4}{\omega_0^8 \ell^2} - \frac{ak^3 M}{\omega_0^6 \ell^2} - \frac{3akMQ^2}{2\omega_0^2 \ell^2} - \frac{2akM}{\omega_0^2}\right) \frac{1}{r^4} \\
&+ \left(3aMQ^2 - \frac{2ak^5}{\omega_0^{10} \ell^2} - \frac{ak^4 M}{\omega_0^8 \ell^2} - \frac{3ak^2 MQ^2}{2\omega_0^4 \ell^2} - \frac{2ak^2 M}{\omega_0^4} + \frac{2akQ^2}{\omega_0^2}\right) \frac{1}{r^5} \\
&+ O\left(M^2, Q^3, a, \frac{1}{\ell^2}\right). \tag{5.7}
\end{aligned}$$

Integrating this expression, we obtain

$$\begin{aligned}
\int_S^R k_g dl &= -\frac{2a}{\ell^2} \left(\frac{\sqrt{1-(bu_R)^2}}{u_R} + \frac{\sqrt{1-(bus)^2}}{u_S}\right) \\
&+ \left(-\frac{2ak}{\omega_0^2 \ell^2} - \frac{aM}{\ell^2}\right) \left(\pi - \arctan(\sqrt{1-(usb)^2}) - \arctan(\sqrt{1-(u_Rb)^2})\right) \\
&- \left(\frac{2ak^2}{\omega_0^4 \ell^2} + \frac{akM}{\omega_0^2 \ell^2}\right) \left(\frac{\pi - \arcsin(bus) + \arcsin(bu_R)}{b}\right) \\
&+ \left(-2aM - \frac{2ak^3}{\omega_0^6 \ell^2} - \frac{ak^2 M}{\omega_0^4 \ell^2} - \frac{3aMQ^2}{2\ell^2}\right) \left(\frac{\sqrt{1-(bus)^2} + \sqrt{1-(bu_R)^2}}{b^2}\right) \\
&+ \left(2aQ^2 - \frac{2ak^4}{\omega_0^8 \ell^2} - \frac{ak^3 M}{\omega_0^6 \ell^2} - \frac{3akMQ^2}{2\omega_0^2 \ell^2} - \frac{2akM}{\omega_0^2}\right) \\
&\times \left(\frac{u_S \sqrt{1-(usb)^2} + u_R \sqrt{1-(u_Rb)^2}}{2b^2} + \frac{\pi - \arcsin(bus) + \arcsin(bu_R)}{2b^3}\right) \\
&+ \left(3aMQ^2 - \frac{2ak^5}{\omega_0^{10} \ell^2} - \frac{ak^4 M}{\omega_0^8 \ell^2} - \frac{3ak^2 MQ^2}{2\omega_0^4 \ell^2} - \frac{2ak^2 M}{\omega_0^4} + \frac{2akQ^2}{\omega_0^2}\right) \\
&\times \left(\frac{u_S^2 \sqrt{1-(usb)^2} + u_R^2 \sqrt{1-(u_Rb)^2}}{3b^2} + \frac{2\left(\sqrt{1-(bus)^2} + \sqrt{1-(bu_R)^2}\right)}{3b^4}\right) \\
&+ O\left(M^2, Q^3, a, \frac{1}{\ell^2}\right). \tag{5.8}
\end{aligned}$$

Combining Eq.(5.6) and Eq.(5.8) in linear approximations, we can get the deflection angle of the Kerr AdS black hole in such a medium. Taking $bus \ll 1$ and $bu_R \ll 1$, we obtain this optical quantity

$$\begin{aligned}
\Theta &= \Theta_{KNAdS} - \frac{8ak^5}{3b^4 \omega_0^{10} \ell^2} - \frac{4ak^4 M}{3b^4 \omega_0^8 \ell^2} - \frac{2ak^2 MQ^2}{b^4 \omega_0^4 \ell^2} - \frac{8ak^2 M}{3b^4 \omega_0^4} + \frac{8akQ^2}{3b^4 \omega_0^2} - \frac{\pi ak^4}{b^3 \omega_0^8 \ell^2} - \frac{\pi ak^3 M}{2b^3 \omega_0^6 \ell^2} \\
&- \frac{3\pi akMQ^2}{4b^3 \omega_0^2 \ell^2} - \frac{\pi akM}{b^3 \omega_0^2} - \frac{4ak^3}{b^2 \omega_0^6 \ell^2} - \frac{2ak^2 M}{b^2 \omega_0^4 \ell^2} - \frac{2\pi ak^2}{b\omega_0^4 \ell^2} - \frac{\pi akM}{b\omega_0^2 \ell^2} - \frac{\pi ak}{\omega_0^2 \ell^2} + \frac{24k^5}{b^3 \omega_0^{10} \ell^2} - \frac{128k^4 M}{3b^3 \omega_0^8 \ell^2} \\
&+ \frac{64k^3 Q^2}{3b^3 \omega_0^6 \ell^2} + \frac{16k^3}{3b^3 \omega_0^6} - \frac{16k^2 M}{b^3 \omega_0^4} + \frac{8kQ^2}{b^3 \omega_0^2} - \frac{9\pi k^4}{4b^2 \omega_0^8 \ell^2} + \frac{33\pi k^3 M}{8b^2 \omega_0^6 \ell^2} - \frac{9\pi k^2 Q^2}{4b^2 \omega_0^4 \ell^2} - \frac{3\pi k^2}{8b^2 \omega_0^4} + \frac{9\pi kM}{8b^2 \omega_0^2} \\
&- \frac{11k^3}{b\omega_0^6 \ell^2} + \frac{22k^2 M}{b\omega_0^4 \ell^2} - \frac{14kQ^2}{b\omega_0^2 \ell^2} - \frac{k}{b\omega_0^2} + \frac{bk}{4\omega_0^2 \ell^2} + \frac{3\pi k^2}{\omega_0^4 \ell^2} - \frac{15\pi kM}{2\omega_0^2 \ell^2} + O\left(M^2, Q^3, a, \frac{1}{\ell^2}\right). \tag{5.9}
\end{aligned}$$

At this level, we could provide certain comments. Taking $k = 0$, we recover the result of the ordinary solutions $\Theta = \Theta_{KN_{AdS}}$. As usually, it follows that the deflection angle expression involves a refractive index contribution. To investigate the effect of the plasma medium on the deflection angle of RN-AdS black holes, we consider as previously two AdS radius values. In particular, we vary the following frequency ratio $\frac{k}{\omega_0^2}$ from 0 to 1. Indeed, Fig(4) illustrates such behaviors. The left and the right panels of this figure show that the deflection angle of light rays remains a decreasing function in terms of the fraction frequency quantity by preserving the same contribution even with large values of b . In the right panel where the AdS space-time contribution is visualized by taking $\ell = 20$, the deflection angle increases for large impact parameter values. This behavior could be explained by the presence of the cosmological constant. This can affect certain parameters as the charge. However, the rotation parameter and the frequency ratio keep the same behaviors for large and small values of the impact parameter in the presence of the AdS space-time.

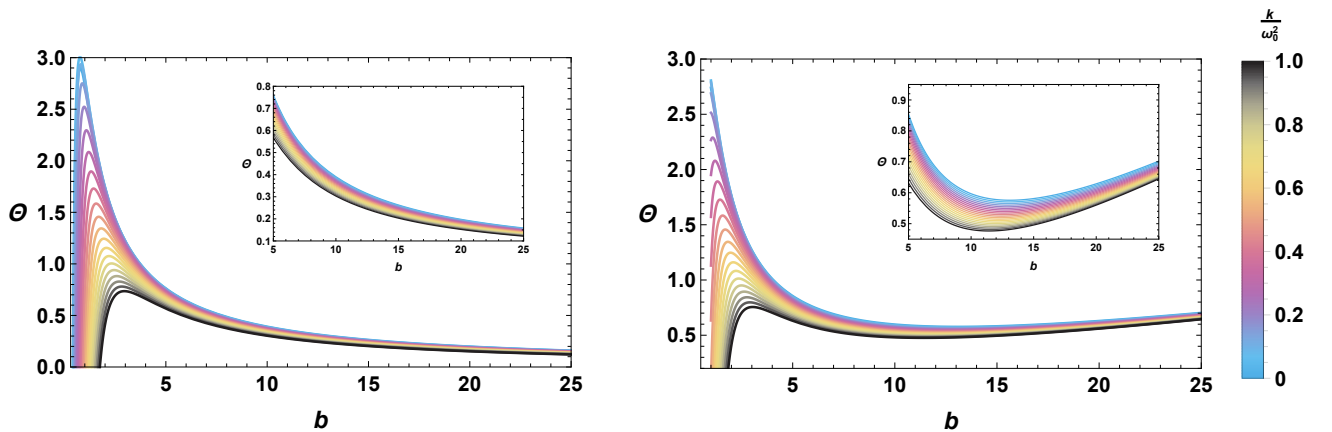


Figure 4: Variation of the deflection angle in terms of the frequency ratio $\frac{k}{\omega_0^2}$ for $u_S = u_R = 0.1$, $Q = 0.2$, $a = 0.2$ and $M = 1$. Left panel: behavior with $\ell = \infty$, right panel: behavior with $\ell = 20$.

6 Conclusions

In this work, we have investigated the deflection angle of AdS black holes in four dimensions. In particular, we have examined the dependence of such a quantity in terms of black hole parameters. Presenting the needed formalism using the Gauss-Bonnet theorem, we have first computed the deflection angle of RN-AdS black holes. In such a model, we have shown that the deflection angle is a decreasing function of the charge and the AdS radius. It has been observed that the deflection angle involves a maximum. This maximum has been increasing by decreasing the charge Q . In particular, we have found a specific point where the behavior of the deflection angle in terms of the charge changes from a decreasing function to an

increasing one. After that, we have studied optical aspects of the Kerr-Newman AdS black holes using the deflection angle variations. Precisely, we have remarked that the behavior of the deflection angle, as a decreasing function of the rotating parameter, does not change in the presence of the AdS space.

Motivated by observational aspects of the plasma influence on the deflection angle being studied by exploiting several astrophysical scenarios, we have inspected the plasma medium effect. Concretely, we have considered the variation of the frequency ratio. Among others, we have remarked that the deflection angle is an increasing function in terms of the ratio $\frac{k}{\omega_0^2}$. At this level, we have observed that, in the plasma medium presence, the deflection angle keeps the same behavior appearing in the rotating black hole with AdS geometries.

This work comes up with certain open questions. Higher dimensional models could be a possible extension of the present work. Dark energy and dark matter effects could be also implemented. We hope address such questions in future works.

Data availability

Data sharing is not applicable to this article.

Acknowledgments

The authors would like to thank H. El Moumni, Y. Hassouni and M. B. Sedra for collaborations on related topics. They are also grateful to the anonymous referee for insightful comments and suggestions. This work is partially supported by the ICTP through AF.

References

- [1] R. Emparan, H. S. Reall, *Black Holes in Higher Dimensions*, Living Rev. Relativity, **11**(1) (2008) 6, [arXiv:0801.3471](#).
- [2] S. W. Hawking, *Black hole explosions*, Nature **248** (1974) 30.
- [3] J. L. Synge, *Relativity: The General Theory*. North Holland, Amsterdam (1960).
- [4] B. Abbott and al., *Observation of Gravitational Waves from a Binary Black Hole Merger*, Phys. Rev. Lett. **116** (6) (2016) 061102, [arXiv:1602.03837](#).
- [5] K. Akiyama and al., *First M87 Event Horizon Telescope Results. IV. Imaging the Central Supermassive Black Hole*, Astrophys. J. **L4** (1) (2019) 875, [arXiv:1906.11241](#).
- [6] K. Akiyama and al., *First M87 Event Horizon Telescope Results. V. Imaging the Central Supermassive Black Hole*, Astrophys. J. **L5** (1) (2019) 875.
- [7] K. Akiyama and al., *First M87 Event Horizon Telescope Results. VI. Imaging the Central Supermassive Black Hole*, Astrophys. J. **L6** (1) (2019) 875.

- [8] Y. Liu, D. C. Zou, B. Wang, *Signature of the Van der Waals like small-large charged AdS black hole phase transition in quasinormal modes*, JHEP. **09** (2014) 179, [arXiv:1405.2644](#).
- [9] A. Belhaj, M. Chabab, H. El Moumni, K. Masmam, M. B. Sedra, A. Segui, *On heat properties of AdS black holes in higher dimensions*, JHEP. **05** (2015) 149, [arXiv:1503.07308](#).
- [10] A. Belhaj, M. Chabab, H. El Moumni, L. Medari, M. B. Sedra, *The thermodynamical behaviors of Kerr–Newman AdS black holes*, CPL. **30** (2013) 090402, [arXiv:1307.7421](#).
- [11] D. Kubizňák, R. B. Mann, Mae Teo, *Black hole chemistry: thermodynamics with Lambda*, Class. Quantum Grav. **34** (2017) 063001, [arXiv:1608.06147](#).
- [12] A. Rajagopal, D. Kubiznak, R. B. Mann, *Van der Waals black hole*, Phys. Lett. B **737** (2014) 277, [arXiv:1408.1105](#).
- [13] S. W. Hawking, D. N. Page, *Thermodynamics of black holes in anti-de Sitter space*, Commun. Math. Phys. **87** (4) (1983) 577.
- [14] Y-Y. Wang, B-Y Su, N. Li, *Hawking Page phase transitions in four-dimensional Einstein Gauss-Bonnet gravity*, Phys. Dark Universe **31** (2021) 100769, [arXiv:2008.01985](#).
- [15] H. Quevedo, A. Sanchez, S. Taj, A. Vazquez, *Phase transitions in geometrothermodynamics*, Gen. Rel. Grav **43** (2011) 1153, [arXiv:1010.5599](#).
- [16] A. Belhaj, M. Chabab, H. El Moumni, M. B. Sedra, *On thermodynamics of AdS black holes in arbitrary dimensions*, CPL. **29** (2012) 100401, [arXiv:1210.4617](#).
- [17] P. V. Cunha, C. A. R. Herdeiro, B. Kleihaus, J. Kunz, E. Radu, *Shadows of Einstein–dilaton–Gauss–Bonnet black holes*, Phys. Lett. B **768**(2017)373, [arXiv:1701.00079](#).
- [18] A. Övgün, I. Sakalli, J. Saavedra, *Shadow cast and Deflection angle of Kerr-Newman-Kasuya spacetime*, JCAP. **10** (2018) 041, [arXiv:1807.00388](#).
- [19] A. Belhaj, H. Belmahi, M. Benali, W. El Hadri, H. El Moumni, E. Torrente-Lujan, *Shadows of 5D Black Holes from string theory*, Phys. Lett. B **812** (2021) 136025, [arXiv:2008.13478](#).
- [20] R. Konoplya, *Shadow of a black hole surrounded by dark matter*, Phys. Lett. B **795** (2019) 1, [arXiv:1905.00064](#).
- [21] S. U. Khan, J. Ren, *Shadow cast by a rotating charged black hole in quintessential dark energy*, Phys. Dark Univ. **30** (2020) 100644, [arXiv:2006.11289](#).

- [22] X. Hou, Z. Xu, J. Wang, *Rotating black hole shadow in perfect fluid dark matter*, JCAP **12** (2018) 040.
- [23] S. W. Wei, Y. C. Zou, Y. X. Liu, R. B. Mann, *Curvature radius and Kerr black hole shadow*, JCAP **08** (2019) 030, [arXiv:1904.07710](#).
- [24] W. Javed, J. Abbas, A. Övgün, *Effect of the quintessential dark energy on weak deflection angle by Kerr Newmann Black hole*, Annals of Physics **418** (2020) 168183, [arXiv:2007.16027](#).
- [25] J. R. Villanueva, J. Saavedra, M. Olivares, N. Cruz, *Photons motion in charged Anti-de Sitter black holes*, Astrophys. Space Sci. **344** (2) (2013) 437.
- [26] W. Javed, M. B. Khadim, J. Abbas, A. Övgün, *Weak gravitational lensing by stringy black holes*, Eur. Phys. J. Plus **3** (2020) 135, [arXiv:2004.00408](#)
- [27] A. Belhaj, M. Benali, A. El Balali, H. El Moumni, S-E. Ennadifi, *Deflection angle and shadow behaviors of quintessential black holes in arbitrary dimensions*, Class. Quantum Grav. **37** (2020) 215004, [arXiv:2006.01078](#).
- [28] R. Uniyal, H. Nandan, P. Jetzer, *Bending angle of light in equatorial plane of Kerr–Sen Black Hole*, Phys. Lett. B **782** (2018) 185, [arXiv:1803.04268](#).
- [29] G. W. Gibbons, M. C. Werner, *Applications of the Gauss–Bonnet theorem to gravitational lensing*, Class. Quantum Grav. **25** (23) (2008) 235009, [arXiv:0807.0854](#).
- [30] W. Javed, J. Abbas, A. Övgün, *Deflection angle of photon from magnetized black hole and effect of nonlinear electrodynamics*, Eur. Phys. J. C, **79** (2019) 694, [arXiv:1908.09632](#).
- [31] G. W. Gibbons, M. Vyska, *The application of Weierstrass elliptic functions to Schwarzschild null geodesics*, Class. Quantum Grav. **29** (2012) 065016, [arXiv:1110.6508](#).
- [32] A. Belhaj, H. Belmahi, M. Benali, A. Segui, *Thermodynamics of AdS black holes from deflection angle formalism*, Phys. Lett. B **817** (2021) 136313.
- [33] T. Ono, A. Ishihara, H. Asada, *Gravitomagnetic bending angle of light with finite-distance corrections in stationary axisymmetric spacetimes*, Phys. Rev. D **96** (2017) 104037, [arXiv:1704.05615](#).
- [34] R. Kumar, S. G. Ghosh, A. Wang, *Shadow cast and deflection of light by charged rotating regular black holes*, Phys. Rev. D **100** (2019) 124024, [arXiv:1912.05154](#).
- [35] A. Ishihara, Y. Suzuki, T. Ono, T. Kitamura, H. Asada, *Gravitational bending angle of light for finite distance and the Gauss-Bonnet theorem*, Phys. Rev. D **94** (2016) 084015, [arXiv:1604.08308](#)

- [36] B. E. Panah, K. Jafarzade, S. H. Hendi, *Charged 4D Einstein-Gauss-Bonnet-AdS Black Holes: Shadow, Energy Emission, Deflection Angle and Heat Engine*, Nucl. Phys. B **961** (2020) 115269, [arXiv:2004.04058](#).
- [37] M. M. Caldarelli, G. Cognola, D. Klemm, *Thermodynamics of Kerr-Newman-AdS Black Holes and Conformal Field Theories*, Class. Quant. Grav. **26** (2009) 195011, [arXiv:hep-th/9908022](#).
- [38] P. Sharma, H. Nandan, R. Gannouji, R. Uniyal, A. Abebe, *Deflection of light by a rotating black hole surrounded by “quintessence”*, Int. J. Mod. Phys. A **35** (2020) 2050155, [arXiv:1911.00372](#).
- [39] R. Adam, *Frequency-dependent effects of gravitational lensing within plasma*, Monthly Notices of the Royal Astronomical Society, **451** (2015) 4536, [arXiv:1505.06790](#).
- [40] A. Abdujabbarov, B. Toshmatov, Z. Stuchlik, B. Ahmedov, *Shadow of the rotating black hole with quintessential energy in the presence of plasma*, Int. J. Mod. Phys. D **26** (2016) 1750051, [arXiv:1512.05206](#).